RAA 2020 Vol. **20** No. **4**, 59(10pp) doi: 10.1088/1674–4527/20/4/59

http://www.raa-journal.org *http://iopscience.iop.org/raa*

***R**esearch in*
***A**stronomy and*
***A**strophysics*

Study of the puzzling abundance pattern of the neutron-capture elements in LMC star J053253.51–695915.1

Wan-Qiang Han[1,2], Lu Zhang[3], Guo-Chao Yang[4], Wen-Yuan Cui[1], Fang Wen[1] and Bo Zhang[1]

[1] Department of Physics, Hebei Normal University, Shijiazhuang 050024, China; *zhangbo@hebtu.edu.cn*
[2] Department of Physics, Shijiazhuang University, Shijiazhuang 050035, China
[3] College of Mathematics and Information Science, Hebei Normal University, Shijiazhuang 050024, China
[4] School of Sciences, Hebei University of Science and Technology, Shijiazhuang 050018, China

Received 2019 September 19, accepted 2020 January 21

Abstract Object J053253.51–695915.1 (J053253) in the Large Magellanic Cloud (LMC) is reported as a young stellar object (YSO). Its chemical abundances reflect the initial composition of the gas cloud in which the star formed. However, the discovery that this star shows the enhancement of the neutron(n)-capture elements and the higher ratio of the heavier n-capture elements relative to the lighter n-capture elements is puzzling. Using an abundance decomposed method, we explore the astrophysical origins of the n-capture elements in this star. We find that the abundance characteristic of the higher ratio of the heavier n-capture elements to the lighter n-capture elements can be explained by the pollution of the r-process event and the contamination of the s-process material.

Key words: stars: abundances — stars: chemically peculiar — stars: individual: J053253.51–695915.1

1 INTRODUCTION

Neutron (n)-capture nucleosynthesis is believed to be responsible for the production of elements heavier than the iron-group elements. There exist two principle n-capture processes: the slow process (s-process) and the rapid process (r-process). The s-process nucleosynthesis contains weak and main components. The weak component occurs in He-burning cores and C-burning shells of the massive stars and mainly produces around the first peak elements. The low to intermediate mass asymptotic giant branch (AGB) stars are the convincing sites of the main component of s-process which generally produces the elements with the mass number $A > 90$ (Busso et al. 1999; Travaglio et al. 2004). The r-process also contains weak and main components. The weak component (or "lighter element primary process") may take place in Type II supernovae (SNe II) with the initial mass range $M \geqslant 10\,M_{\odot}$ and can be an origin of the light n-capture elements with mass number $A < 130$ (Travaglio et al. 2004; Qian & Wasserburg 2007). The main component of the r-process nucleosynthesis, associating with greatly neutron-rich environment, can produce light and heavy n-capture elements. Several previous studies considered that the astrophysical environment of the r-process associates with SNe II (Travaglio et al. 1999; Qian & Wasserburg 2007). However, recent researchers suggested that neutron star mergers (Tsujimoto et al. 2014; Ji et al. 2016; Komiya & Shigeyama 2016) should be the most promising sites, which has now been verified in a general sense by the observation of the kilonova counterpart of the neutron star merger GW 170817 (Cowperthwaite et al. 2017; Drout et al. 2017; Tanvir et al. 2017).

The low and intermediate mass AGB stars with carbon and the s-process elements enhanced in their envelopes can be divided into intrinsic and extrinsic AGB stars (Smith & Lambert 1990; Lambert et al. 1995). For the intrinsic AGB stars, the s-process enrichment in stellar envelopes is produced by dredging up the nucleosynthesis products generated in the stellar interior during their thermal pulse stages. On the other hand, the extrinsic AGB stars are enriched in the s-process elements by the mass transfer from initially more massive stars which have evolved through the thermally pulsing AGB phase and now are white dwarfs (Busso et al. 2001). When the low and intermediate mass AGB stars undergo mass-loss in superwind largely enough, their envelopes would be expelled, and these objects will enter the post-AGB phase which approaches the planetary nebula phase (Van Winckel 2003; De Smedt et al. 2015).

Through studying the elemental abundances of the post-AGB stars in the Large Magellanic Cloud (LMC), van Aarle et al. (2013) found that, compared to other post-AGB stars in the LMC, star J053253.51–695915.1 (J053253) exhibits different abundance characteristics: a higher neutron exposure efficiency and a lower s-process enhancement. van Aarle et al. (2013) reported that the subluminosity and the deviation of the s-process pattern from the other post-AGB stars are difficult to be explained by the single-star evolution track. They suggested that J053253 may be enriched in s-process elements through mass transfer in the binary system and possesses extrinsic feature. However, they also pointed that the dust excess observed for J053253 is not the characteristic of the extrinsic objects. Based on a $\log g$ criterion, Kamath et al. (2015) classified J053253 as a young stellar object (YSO). They suggested that the enhancement of the n-capture elements in this star should be attributed to the initial composition of the LMC. In this case, the explanation about the observed abundance characteristics, such as the enhancement of the n-capture elements and the higher ratio of the heavier n-capture elements relative to the lighter n-capture elements is needed. Obviously, investigating the astrophysical origins of the n-capture elements in this star is an important task. Because the abundance pattern is closely related to nucleosynthesis process, in this work, adopting an abundance decomposed method, we have studied the abundance characteristics of star J053253 and investigate the astrophysical origin of its n-capture elements. In Section 2, we compare the n-capture abundances of J053253 with other post-AGB stars, extreme r-II stars and the r-I star. Our calculations and discussion are presented in Section 3. Section 4 gives our conclusions.

2 THE COMPARISON OF THE N-CAPTURE ENRICHMENT BETWEEN J053253 AND OTHER STARS

We arrive at a challenge to explain logically the abundance characteristics of J053253, a star that was reported as a post-AGB star in LMC by van Aarle et al. (2013) and reclassified as a YSO by Kamath et al. (2015). Figure 1 shows the comparison of the observed ratios [X/Fe] in this star and the averaged ratios [X/Fe] in normal LMC stars (Van der Swaelmen et al. 2013). Using high-resolution spectra, Van der Swaelmen et al. (2013) analyzed the chemical abundances of the LMC field red giant stars in the bar and inner disk of the LMC. As a YSO, the chemical abundances of J053253 would reflect the initial composition of the LMC (Kamath et al. 2015) and the values of [La/Fe] and [Eu/Fe] in this object should be close to those in the LMC. From the figure, we can see that the abundance ratios of the n-capture elements are higher in J053253 than the averaged ratios in the normal LMC stars, particularly, [La/Fe] and [Eu/Fe] are about 0.6 and 0.4 dex respectively higher in J053253 than in the normal LMC stars. In Figure 2, we present the comparison of the abundance ratios [X/Eu] in the sample star with in the solar system (Arlandini et al. 1999). We find that the [X/Eu] ratios in J053253 lie between the solar s-process and solar r-process ratios and near the solar total [X/Eu] ratios, which indicates the n-capture elements of this star might come from the combination of the s- and r-processes. In order to obtain the abundance characteristics of J053253, we will compare the abundance patterns of this star with those of the post-AGB stars, extreme r-II stars and r-I star. Figures 3(a) and (b) display the comparison of the observed [X/Eu] ratios in J053253 with in 8 post-AGB stars and the averaged [X/Eu] ratios of the post-AGB stars. The abundance data of the 8 post-AGB stars are adopted from Van Winckel & Reyniers (2000); Reyniers et al. (2004); van Aarle et al. (2013); De Smedt et al. (2016). We find that, for the most observed n-capture elements, [X/Eu] ratios are higher in post-AGB stars than in this sample star about 0.6 dex (averaged), which implies that the contributions of the s-process to those post-AGB stars are higher than to J053253 relative to Eu. Figures 4(a) and (b) show the comparison of the observed [X/Eu] ratios in J053253 with in the extreme r-II stars stars and the averaged [X/Eu] ratios of the extreme r-II stars. The abundance data of the r-II stars are adopted from Hill et al. (2002); Sneden et al. (2003); Barklem et al. (2005); Frebel et al. (2007); Hayek et al. (2009); Aoki et al. (2010); Placco et al. (2017); Ji et al. (2018). We can see that, for the most n-capture elements, [X/Eu] ratios are lower in the r-II stars than in the sample star about 0.5 dex (averaged). In Figure 5, we performed the comparison of the ratios [X/Eu] in J053253 with r-I star HD 221170 (Ivans et al. 2006), since their [Eu/Fe] ratios are close. Similar behavior is exhibited in Figure 4.

3 STUDY OF THE ABUNDANCE CHARACTERISTICS AND THE INVESTIGATION OF THE ASTROPHYSICAL ORIGINS OF THE N-CAPTURE ELEMENTS

The stellar abundances provide us very important information to investigate the origin of the elements in the star. To study the origin of the elements in the sample star, we follow the model by Li et al. (2013b) assuming that the abundance of the ith element in star J053253 (N_i) originates from five components (the main r-, primary, main s-, secondary processes, and SNe Ia). The model can be ex-

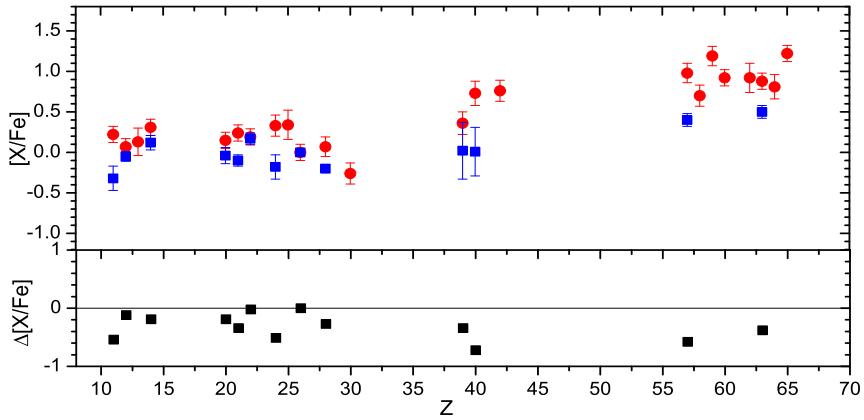

Fig. 1 Comparison between the observed ratios [X/Fe] in J053253 and the averaged ratios [X/Fe] in normal LMC stars. The *filled squares* (*blue*) represent the averaged ratios of the normal LMC stars (Van der Swaelmen et al. 2013) and the *filled circles* (*red*) represent the observed ratios of J053253 (van Aarle et al. 2013). The lower panel shows the deviation of the averaged ratios [X/Fe] in LMC from those of the sample star.

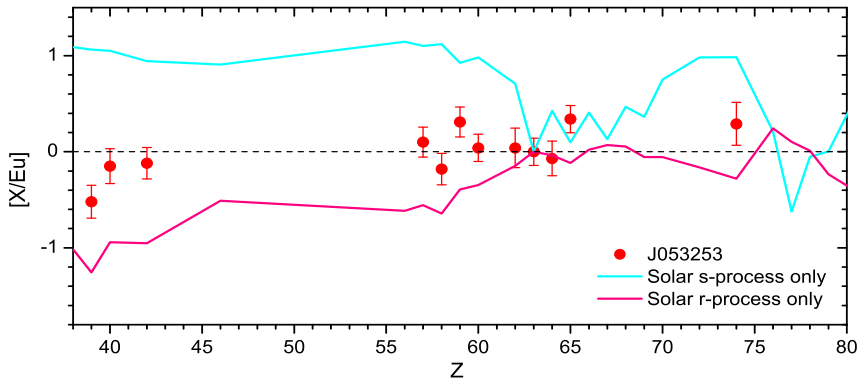

Fig. 2 Comparison of the observed abundance ratios [X/Eu] in J053253 with the solar s- and solar r-process ratios. The *curved lines* represent the solar s-process only ratios (*cyan*) (Arlandini et al. 1999) and the solar r-process only ratios (*pink*) (Li et al. 2013a). The *dashed line* indicates the solar total ratios. The *filled* (*red*) *circles* represent the ratios of J053253 (van Aarle et al. 2013).

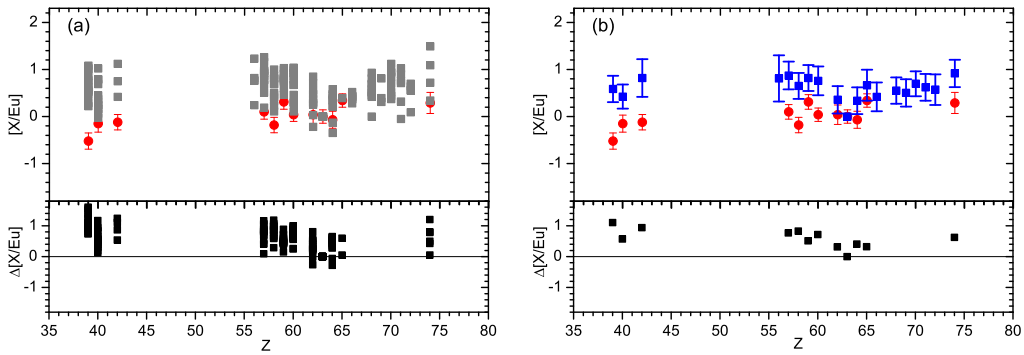

Fig. 3 (a) *Upper*: Comparison of the abundance ratios [X/Eu] in J053253 with those in the post-AGB stars. The *filled* (*red*) *circles* represent the observed [X/Eu] ratios of J053253. The *gray squares* indicate the data of the post-AGB stars which are adopted from Van Winckel & Reyniers (2000); Reyniers et al. (2004); van Aarle et al. (2013); De Smedt et al. (2016). *Lower*: The deviations of the ratios in post-AGB stars from in the sample star. (b)*Upper*: Comparison of the [X/Eu] ratios in J053253 with the averaged [X/Eu] ratios of the post-AGB stars. The *blue squares with the error bars* represent the averaged values. *Lower*: The deviations of the averaged ratios of post-AGB stars from the [X/Eu] ratios in the sample star.

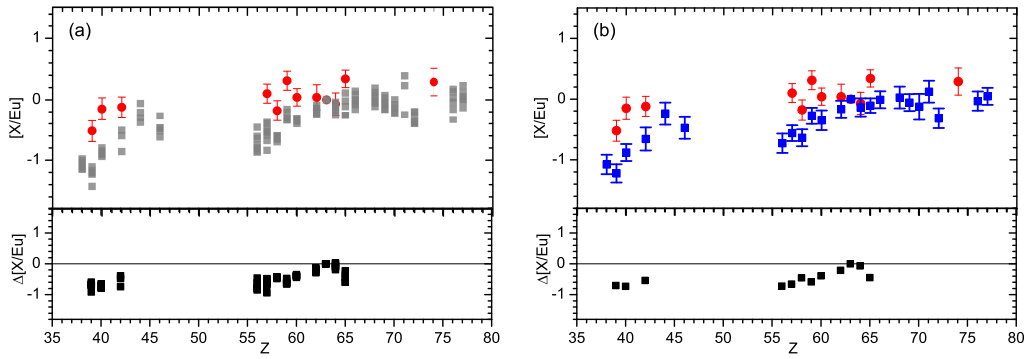

Fig. 4 (a) *Upper*: Comparison of the abundance ratios [X/Eu] in J053253 with the extreme r-II stars. The *gray squares* indicate the observed ratios of the r-II stars with [r/Fe]$\geq$ 1.5. The data of r-II stars are taken from Hill et al. (2002); Sneden et al. (2003); Barklem et al. (2005); Frebel et al. (2007); Hayek et al. (2009); Aoki et al. (2010); Placco et al. (2017); Ji et al. (2018). *Lower*: The deviations of the ratios in the r-II stars from that for the sample star. (b) *Upper*: Comparison of the [X/Eu] ratios in J053253 with the averaged [X/Eu] ratios of the extreme r-II stars. The *blue squares with the error bars* represent the averaged values. *Lower*: The deviations of the averaged ratios of r-II stars from the [X/Eu] ratios for the sample star.

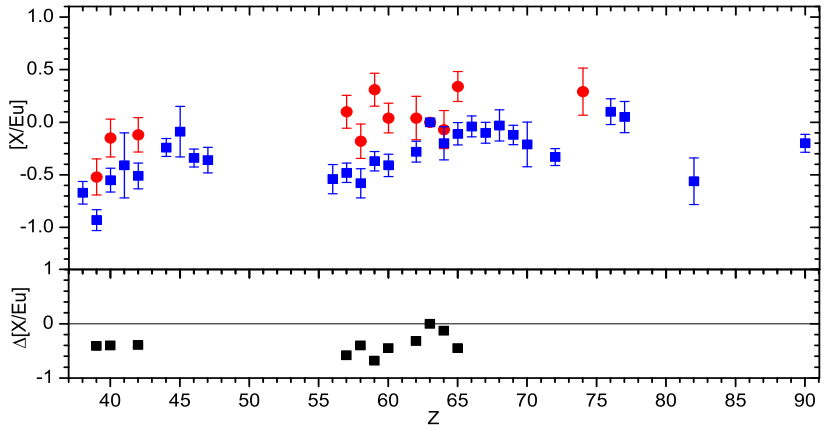

Fig. 5 Comparison of the abundance ratios [X/Eu] between J053253 and r-I star HD 221170. The abundance data of HD 221170 are adopted from Ivans et al. (2006).

pressed as:

$$N_i = (C_{r,m}N_{i,r,m} + C_{\rm pri}N_{i,\rm pri} + C_{s,m}N_{i,s,m} + C_{\rm sec}N_{i,\rm sec} + C_{\rm ia}N_{i,\rm Ia}) \times 10^{[\rm Fe/H]}, \quad (1)$$

where $N_{i,r,m}$, $N_{i,\rm pri}$, $N_{i,s,m}$, $N_{i,\rm sec}$, and $N_{i,\rm Ia}$ indicate the corresponding component abundances which have been scaled to the corresponded component abundances of the solar system. $C_{r,m}$, $C_{\rm pri}$, $C_{s,m}$, $C_{\rm sec}$, and $C_{\rm Ia}$ are the coefficients which represent the relative contributions of the corresponding components. These coefficients can be derived by comparing the calculated abundances with the observed abundances and looking for the smallest χ^2. The value of $N_{i,\rm Ia}$ is referenced from Timmes et al. (1995). $N_{i,r,m}$ and $N_{i,\rm pri}$ are taken from Li et al. (2013a). Because both the primary light elements and weak r-process elements are ejected from massive stars, $N_{i,\rm pri}$ includes the abundances of the primary light elements and weak r-process elements. Similarly, $N_{i,\rm sec}$ includes the abundances of the secondary light elements and weak s-process elements, because these elements originate from massive stars. The component abundances of the secondary process are adopted from Li et al. (2013a). The weak s-process abundances are taken from Raiteri et al. (1993). Based on the nucleosynthesis calculations, Bisterzo et al. (2010) presented a set of AGB yields of low-mass and low metallicity for various ^{13}C-pocket efficiencies, including the standard case (hereafter ST), ST/6, ST/12 and ST/24. For the ST case adopted by Gallino et al. (1998), the low-mass AGB stars at half solar metallicity can exactly explain the main component of the solar s-process abundances (Arlandini et al. 1999). Adopting the AGB yields presented by Bisterzo et al. (2010), the scaled abundances of $N_{i,s,m}$ is calculated as the combination of the ST case and the ST/12 case with the $M = 1.5\ M_\odot$ at [Fe/H]$= -1.0$:

$$C_{s,m}N_{i,s,m} = C_1 N_{i,s,m}(\rm ST) + C_2 N_{i,s,m}(\rm ST/12), \quad (2)$$

where $N_{i,s,m}$, $N_{i,s,m}$(ST) and $N_{i,s,m}$(ST/12) are scaled to the Ba abundance of the solar s-process. C_1 and C_2 indi-

cate the relative contributions of the ST case and the ST/12 case to the main s-process. For the best-fitted results, the value of χ^2 is 0.517, the derived coefficients are $C_{r,m} = 13.40, C_{\rm pri} = 1.30, C_1 = 5.10, C_2 = 0.40$ ($C_{s,m} = 5.50$), $C_{\rm sec} = 1.50$, and $C_{\rm Ia} = 0.8$, respectively. In the calculations, the abundances of s-process are obtained from the expression $C_1 N_{i,s,m}$(ST)+$C_2 N_{i,s,m}$(ST/12), which means that the abundances of s-process are dependent on C_1, C_2, $N_{i,s,m}$(ST) and $N_{i,s,m}$(ST/12). If we change the representative element from Ba to other element (such as La), the scaled s-process abundances ($N_{i,s,m}$(ST) and $N_{i,s,m}$(ST/12)) should change, then the values of C_1 and C_2 ($C_{s,m} = C_1 + C_2$ is valid for La) should also change. This guarantees that the calculated abundances of s-process from the expression do not change, because the best fitted result from Equation (1) does not change. In this work, the equation $C_{s,m} = C_1 + C_2$ is valid for Ba, since $N_{i,s,m}$, $N_{i,s,m}$(ST) and $N_{i,s,m}$(ST/12) are scaled to the Ba abundance of the solar s-process. The derived $C_{r,m}$ and $C_{s,m}$ are larger than other coefficients, which indicates that the star exhibits significant s- and r-process characteristics. The comparisons of the calculated abundances with the observed abundances are plotted in Figure 6. We can see that, for the most elements, the calculations are consistent with the observations within the uncertainties. To study the astrophysical origins of each element in the sample star, Figure 7 shows the calculated abundance ratios and components ratios of the elements of the sample star. For comparison, the observed abundance ratios are also shown. Because the calculated abundance uncertainties come from the observed uncertainties, for simplicity, we adopt the mean of the observed uncertainties as the calculated uncertainties, which is about 0.13 dex. From the figure, we find that the light elements Mg, Si, and Ca are mainly produced by the primary process, and Na, Al, Sc, Cr, Mn, and Ni are mainly produced by the secondary process of the massive stars. Element Fe is mainly produced by SNe Ia, and Ti mainly comes from the mixture of the secondary process and SNe Ia. For the lighter n-capture elements, Y is mainly produced by the main s-process, and elements Zr and Mo mainly originate from the combined main s-process and the main r-process. For the heaviest elements beyond La, the main s-process dominates the production of La and Ce, while the main r-process dominates the production of elements Sm, Eu, Gd, and Tb. In addition, element Pr, Nd, and W own their origins to the mixture of the main s- and the main r-processes.

van Aarle et al. (2013) reported that J053253 exhibits a higher ratio of the heavier n-capture elements (La, Nd, Sm) relative to the lighter n-capture elements (Y, Zr) and lower enrichment of n-capture elements compared to post-AGB stars. Similar to van Aarle et al. (2013), we define [s/Fe] as the mean of [Y/Fe], [Zr/Fe], [Ba/Fe], [La/Fe], [Nd/Fe] and [Sm/Fe], and the index [hs/ls] represents the difference between the mean of [Ba/Fe], [La/Fe], [Nd/Fe] and [Sm/Fe] and the mean of [Y/Fe] and [Zr/Fe]. Because of no observed Ba abundance for J053253 (see van Aarle et al. 2013), its hs-index does not contain Ba abundance. In Figure 8, we present the comparison of [hs/ls] between the sample star and the post-AGB stars. The green squares indicate the post-AGB stars adopted by van Aarle et al. (2013), and their linear least-squares fit line is also displayed. From the figure we can see that our calculation (blue star) is close to the observed ratio (red circle) of J053253.

Based on the abundance analysis, van Aarle et al. (2013) found that the abundances of J053253 are different from those of other post-AGB stars. For J053253, the observed [hs/ls] ratio of this star is 0.39 ± 0.14 which is higher than those of other post-AGB stars with similar s-process enhancement. However, the [s/Fe] ratio is 0.78 ± 0.14 which is lower than those of other post-AGB stars. Based on our calculations, the n-capture elements Y, Zr, La, Ce, Nd in J053253 contain the contributions of the r-process. In order to understand the observed abundance characteristics, we define the component ratios of the s-process and the r-process as

$$[{\rm El}_i/{\rm Fe}]_k = \log(N_{i,k}) - \log(N_{i,\odot}), \qquad (3)$$

where $k = r, s$. $N_{i,k}$ is the abundance of the ith element in J053253, and $N_{i,\odot}$ is the abundance of the ith element in the solar system. The calculated component ratios of $[{\rm hs/ls}]_r$ and $[{\rm hs/ls}]_s$ are about 0.65 and 0.31 which are shown in Figure 9 by the horizontal solid line and the horizontal dashed line, respectively. It can be seen from the figure that the abundance ratio of [hs/ls] in J053253 lies between the ratios of the r-process component and the s-process component. Obviously, the higher ratio of the heavier n-capture elements relative to the lighter n-capture elements for J053253 can be understood by the mixture of the r-process and the s-process. The calculated component ratios of $[{\rm s/Fe}]_r$ and $[{\rm s/Fe}]_s$ are about 0.45 and 0.44 which are shown in the figure by the vertical solid line and the vertical dashed line, respectively. We can see that the component ratios of the r-process and s-process are both lower than the abundance ratio of J053253. The lower abundance ratio [s/Fe] can be explained by the combined contributions of the r-process and the s-process.

Obviously, the abundance difference between star J053253 and the normal LMC stars contains useful information about the chemical enhancement of the gas cloud in which J053253 formed. Based on our calculations, we suggest that, for the gas cloud in which J053253 formed, the enrichment could be divided into two steps. Firstly, the

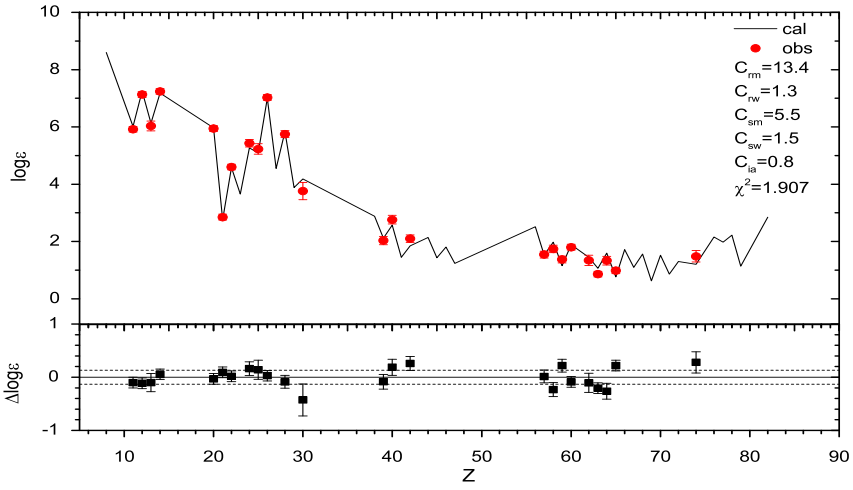

Fig. 6 *Upper*: The comparisons of calculated results with the observations. The observed abundances are represented by *filled circles* and the calculated abundances are marked as the *solid lines*. The data are taken from van Aarle et al. (2013). *Lower*: The relative offsets ($\Delta \log \varepsilon = \log N_{i,\mathrm{obs}} - \log N_{i,\mathrm{cal}}$) and the observed uncertainties.

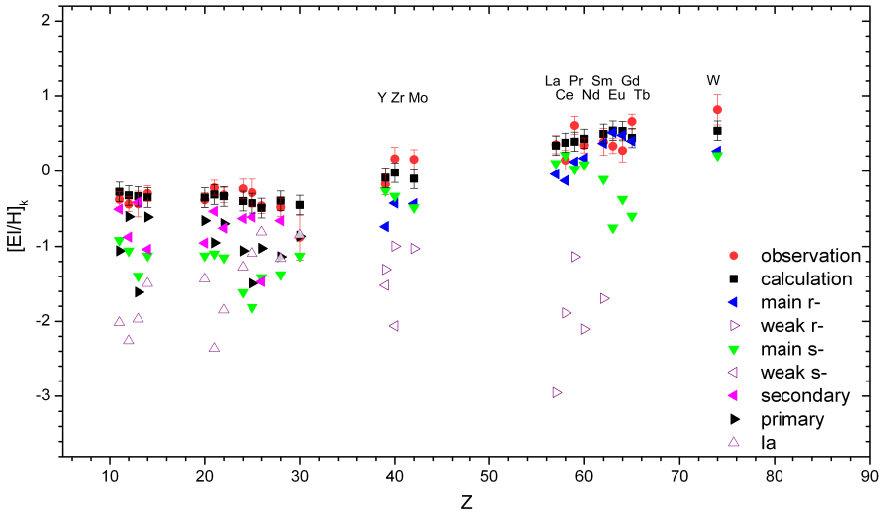

Fig. 7 Component ratios of the individual processes. The *filled circles* are the observed abundance ratios (van Aarle et al. 2013) and the *filled squares* represent the calculated ratios. The *filled right triangles*, *filled left triangles*, *open triangles*, *open right triangles*, *filled down triangles* and *open left triangles* are the ratios of primary, secondary, main r-, weak r-, main s- and weak s-components, respectively.

gas cloud is polluted by the products of the r-process event, and secondly, the gas cloud is contaminated by the s-process products of the low mass AGB stars. Note that the elements La and Ce mainly come from the s-process, and elements Sm, Eu, Gd and Tb mainly originate from the r-process. In Figure 10, we explore the enrichment history from the initial composition of LMC to that of J053253 in [La+Ce/Fe] vs. [Sm+Eu+Gd+Tb/Fe] space. The dashed line and the dash-dotted line indicate the main s-process (Bisterzo et al. 2010) and the solar-r (Li et al. 2013a), respectively. The solid line is [La+Ce/Sm+Eu+Gd+Tb]$= 0$. The black filled star represents the initial composition of the LMC (Van der Swaelmen et al. 2013). The red circle and the blue square represent the observed and the calculated results, respectively.

Komiya & Shigeyama (2016) studied the r-process enrichment by NSM. They suggested that the Eu yield from an NSM event is about $1.5 \times 10^{-4}\ M_{\odot}$ and it can pollute $\sim 10^{7}\ M_{\odot}$ cloud. Recently, Roederer et al. (2018) reported that there are some r-process enhanced stars with high [Fe/H] ratios and suggested that the stars formed in low-mass dwarf galaxy enriched by a high-yield r-process

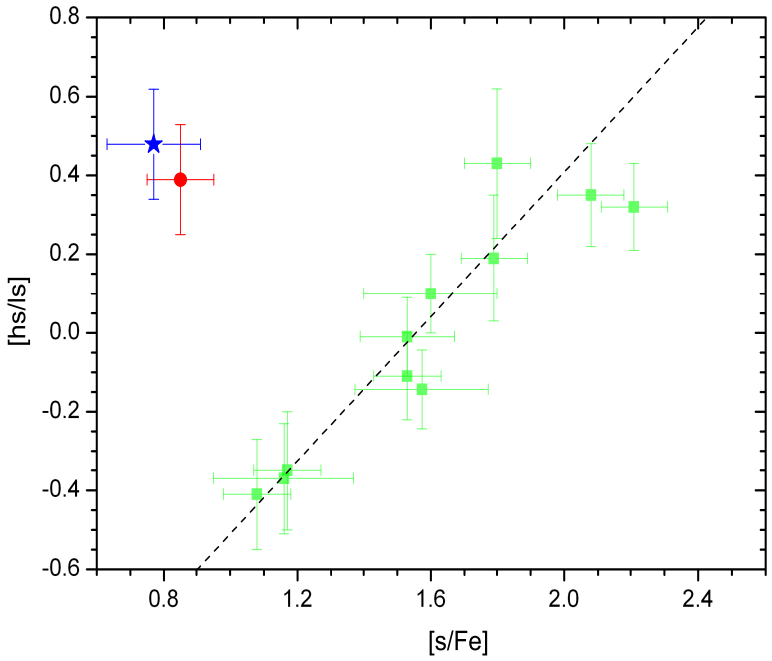

Fig. 8 [hs/ls] vs. [s/Fe] in J053253 and post-AGB stars. The index [s/Fe] is the mean of [Y/Fe], [Zr/Fe], [Ba/Fe], [La/Fe], [Nd/Fe] and [Sm/Fe]. The index [hs/ls] represents the difference between the mean of [Ba/Fe], [La/Fe], [Nd/Fe] and [Sm/Fe] and the mean of [Y/Fe] and [Zr/Fe]. Since no observed Ba abundance for J053253, its hs-index does not contain Ba abundance. The *green squares* represent the post-AGB stars mentioned by van Aarle et al. (2013). The abundance data are adopted from Van Winckel & Reyniers (2000); Reyniers et al. (2004); van Aarle et al. (2013). The *dashed line* is the linear least-squares fit of the post-AGB stars by van Aarle et al. (2013) (see their fig. 9). The *filled circle* (*red*) represents the observed ratio (van Aarle et al. 2013) and the *blue filled star* represents the calculated result of J053253.

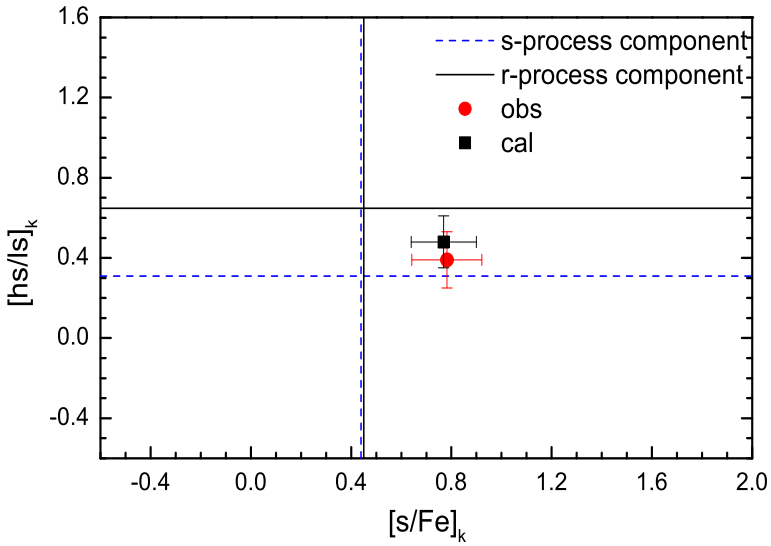

Fig. 9 The comparison of component ratios $[hs/ls]_k$ and $[s/Fe]_k$ with the observed ratio of J053253. The [s/Fe] ratio is the mean of [Y/Fe], [Zr/Fe], [La/Fe], [Nd/Fe] and [Sm/Fe], and the index [hs/ls] represents the difference between the mean of [La/Fe], [Nd/Fe] and [Sm/Fe] and the mean of [Y/Fe] and [Zr/Fe]. The *filled circle* represents the observed ratio, and the *filled square* represents the calculated ratio. The *solid lines* and the *dashed lines* represent the r-process and s-process components, respectively.

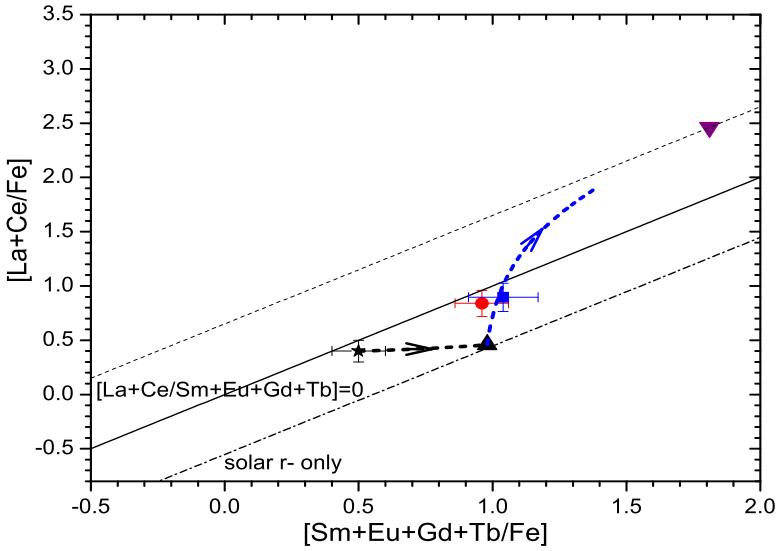

Fig. 10 The enrichment history of J053253 in [La+Ce/Fe] vs. [Sm+Eu+Gd+Tb/Fe] space. For star J053253, the elements La and Ce mainly come from the s-process, and the elements Sm, Eu, Gd and Tb mainly originate from the r-process. The *circle* (*red*) and the *square* (*blue*) represent the observed result (van Aarle et al. 2013) and calculated result of J053253. The *filled star* (*black*) represents the initial composition of the LMC (Van der Swaelmen et al. 2013). The *solid line* is [La+Ce/Sm+Eu+Gd+Tb]$=0$. The *dashed line* and the *dash-dotted line* are corresponding to the main s-process (Bisterzo et al. 2010) and solar-r (Li et al. 2013a), respectively. The *short-dashed blue* and *black lines* represent the pollution track of the main s-process material and the r-process material, respectively. The *triangle* represents the calculated r-process component, and the *down triangle* indicates the ratio of the low mass AGB star from Bisterzo et al. (2010).

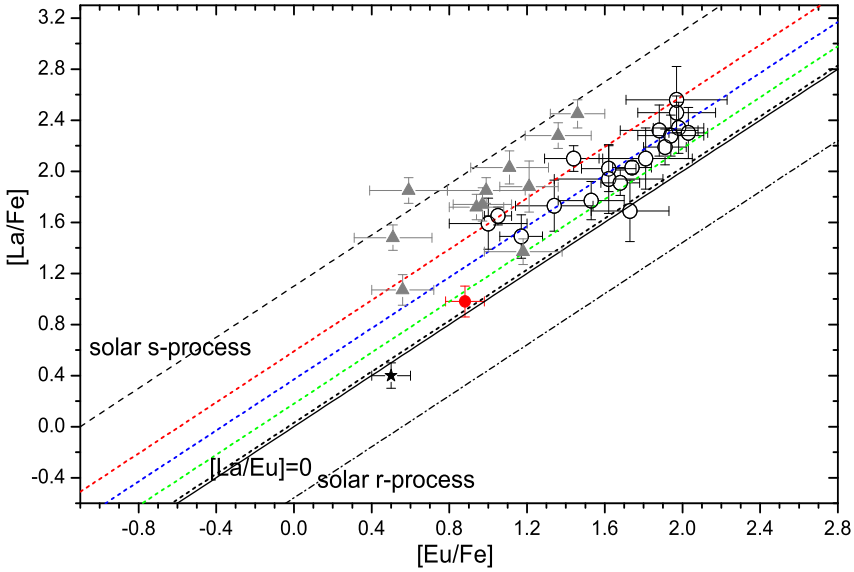

Fig. 11 [La/Fe] vs. [Eu/Fe] in J053253, post-AGB stars and the CEMP-i stars. The CEMP-i stars are indicated as *empty circles*, and the post-AGB stars are indicated as the *gray filled triangles*. The data of CEMP-i stars are taken from Preston & Sneden (2001); Aoki et al. (2002a,b); Cohen et al. (2003, 2006); Johnson & Bolte (2004); Ivans et al. (2005); Barbuy et al. (2005); Barklem et al. (2005); Goswami et al. (2006); Jonsell et al. (2006); Masseron et al. (2010); Allen et al. (2012); Placco (2013), and the data of the post-AGB stars are taken from Van Winckel & Reyniers (2000); Reyniers et al. (2004); van Aarle et al. (2013). The *short dashed lines* with *red*, *blue*, *green* and *black colors* represent the [La/Eu] of the i-process with neutron densities 10^{12}, 10^{13}, 10^{14} and 10^{15} cm^{-3}, respectively (Hampel et al. 2016). The *filled* (*red*) *circle* is star J053253 (van Aarle et al. 2013). The *solid line* is [La/Eu]$=0$. The *dashed line* and the *dash dotted line* are the [La/Eu] of the solar-s only (Arlandini et al. 1999) and solar-r only (Li et al. 2013a), respectively. The *filled star* is the averaged value in LMC (Van der Swaelmen et al. 2013).

event. For a cloud polluted by a r-process event, the abundance relation of Eu and Fe can be expressed as (Yang et al. 2017):

$$N_{\rm Eu}/N_{\rm Fe} = (A_{\rm Fe}/A_{\rm Eu})\cdot(M_{\rm SW}X_{\rm Eu}+Y_{\rm Eu})/(M_{\rm SW}X_{\rm Fe}), \quad (4)$$

where $M_{\rm SW}$ indicates the cloud mass. $A_{\rm Eu}$ and $A_{\rm Fe}$ represent the atomic mass. $X_{\rm Eu}$ and $X_{\rm Fe}$ indicate the initial mass fractions of elements Eu and Fe of the cloud. $Y_{\rm Eu}$ is the r-process yield from an NSM event. For J053253, the [Eu/Fe] ratio is 0.88 and the averaged ratio [Eu/Fe] of the LMC is about 0.5. Adopting the cloud mass $M_{\rm SW} \approx 10^7\ M_{\odot}$, the Eu yield by an NSM event would reach $\sim 5.0 \times 10^{-3}\ M_{\odot}$, which is higher than the Eu yield by Komiya & Shigeyama (2016) about 1.5 order of magnitude. Note that, if the polluted cloud mass is less than $10^7\ M_{\odot}$, it is not necessary that the pollution is from a high-yield r-process event. In Figure 10, the abundances of the gas cloud polluted by the products of the r-process event is indicated as a short-dashed black curve with arrow.

For a gas cloud polluted by the s-process material, the mass abundance of the ith element could be approximately expressed as:

$$X_i \backsimeq X_{i,\rm ini} + f * X_{i,\rm s}, \quad (5)$$

where f is the mass fraction of the s-process material. $X_{i,\rm ini}$ is the abundance which had been polluted by the r-process material, and $X_{i,\rm s}$ is the s-process abundance of the low mass AGB stars. Since the dilution factor of the incorporated s-process material for J053253 is only about 5 percent, the s-process enrichment is mild. In the figure, the abundances of the gas cloud contaminated by the s-process products of the low mass AGB stars is indicated as a short-dashed blue curve with arrow. We can see that the abundance characteristics of the star J053253 can be understood by the pollution of the r-process and the s-process.

The astrophysical origins of the n-capture elements are closely related to the formation scenario of J053253. If J053253 is a post-AGB star or an extrinsic object (e.g., van Aarle et al. 2013), its abundance characteristics of the n-capture elements should be ascribed to the AGB nucleosynthesis. The intermediate n-capture process (i-process) proposed by Cowan & Rose (1977) probably occurs in some circumstance with high neutron density about 10^{15} cm^{-3} in the AGB stars Hampel et al. (2016). Based on the nuclear network calculations, Hampel et al. (2016) calculated the i-process yields at various neutron densities $10^{12}\,{\rm cm}^{-3} - 10^{15}\,{\rm cm}^{-3}$. Using the calculated i-process abundances, Hampel et al. (2016) successfully reproduced the chemical abundances of 19 carbon-enhanced metal-poor (CEMP) stars and named them as CEMP-i stars. In Figure 11, we present the abundance comparison between J053253 and the CEMP-i stars studied by Hampel et al. (2016). The abundance data of the CEMP-i stars indicated by empty circles are taken from Preston & Sneden (2001); Aoki et al. (2002a,b); Cohen et al. (2003, 2006); Johnson & Bolte (2004); Ivans et al. (2005); Barbuy et al. (2005); Barklem et al. (2005); Goswami et al. (2006); Jonsell et al. (2006); Masseron et al. (2010); Allen et al. (2012); Placco (2013). For comparison, the post-AGB stars are also shown by gray triangles. The calculated i-process abundances with neutron densities 10^{12}, 10^{13}, 10^{14} and 10^{15} cm^{-3} by Hampel et al. (2016) are shown in the figure by short dashed lines with red, blue, green, and black, respectively. From the figure, we can see that J053253 is located on the lower end of the CEMP-i stars region in the [La/Fe] vs. [Eu/Fe] space. Meanwhile, the abundance ratios of J053253 are close to those of i-process calculation with 10^{15} cm^{-3}. The comparison results imply that, if J053253 is a post-AGB star or an extrinsic object, the i-process scenario might provide an explanation for the observed characteristics of this star.

4 CONCLUSIONS

We have presented a detailed study of the astrophysical origins of the n-capture elements of LMC star J053253. Using a linear superposition method, we successfully fit the abundance patterns of this star with the combination of five component abundances and the derived coefficients $C_{r,m} = 13.4$, $C_{\rm pri} = 1.3$, $C_{s,m} = 5.5$ ($C_1 = 5.1$, $C_2 = 0.4$), $C_{\rm sec} = 1.5$, and $C_{\rm Ia} = 0.8$, respectively. Our results are given as follows:

The chemical composition would reflect the initial composition of the gas cloud in which the LMC star J053253 formed, since it is a YSO. We find that the α elements Mg, Si and Ca mainly originate from the primary process, and the light elements (e.g., Na, Al, Sc, Cr, Mn and Ni) mainly originate from the secondary process, which indicates that the massive stars make a major contribution to the light elements of J053253. Element Fe in this star mainly comes from SNe Ia. The abundance ratios [La/Fe] and [Eu/Fe] are about 0.5 dex higher in this star than in normal LMC stars, which implies that its n-capture elements should have additional origins. Based on the superposition method, we find that, for J053253, the n-capture abundances can be fitted by the combination of the s- and r-process abundances. The elements Y, La, Ce, Pr and Nd mainly originate from the s-process products of the low mass AGB stars and the elements Eu, Gd and Tb mainly come from the r-process event. The puzzling abundance characteristic of the higher ratio of the heavier n-capture elements to the lighter n-capture elements can be explained by the combination of the s-process and the r-process. Furthermore, the possible pollution tracks for the gas cloud in which J053253 formed are explored. We find

that the astrophysical reasons for the enhancement of the n-capture elements of J053253 can be ascribed to the pollution of the r-process event and the contamination of the s-process material.

We hope that our results in this work can provide more information and more constraints on the study of the astrophysical origins of the n-capture elements of the LMC star.

Acknowledgements We thank the referee for the insightful and constructive suggestions, which improved this paper greatly. This work has been supported by the National Natural Science Foundation of China (Grant Nos. 11673007, 11547041, 11643007 and 11773009), the Natural Science Foundation of Hebei Province (Grant No. A2019208194).

References

Allen, D. M., Ryan, S. G., Rossi, S., Beers, T. C., & Tsangarides, S. A. 2012, A&A, 548, A34
Aoki, W., Norris, J. E., Ryan, S. G., Beers, T. C., & Ando, H. 2002a, PASJ, 54, 933
Aoki, W., Norris, J. E., Ryan, S. G., Beers, T. C., & Ando, H. 2002b, ApJ, 567, 1166
Aoki, W., Beers, T. C., Honda, S., & Carollo, D. 2010, ApJ, 723, L201
Arlandini, C., Käppeler, F., Wisshak, K., et al. 1999, ApJ, 525, 886
Barbuy, B., Spite, M., Spite, F., et al. 2005, A&A, 429, 1031
Barklem, P. S., Christlieb, N., Beers, T. C., et al. 2005, A&A, 439, 129
Bisterzo, S., Gallino, R., Straniero, O., et al. 2010, MNRAS, 404, 1529
Busso, M., Gallino, R., & Wasserburg, G. J. 1999, ARA&A, 37, 239
Busso, M., Gallino, R., Lambert, D. L., et al. 2001, ApJ, 557, 802
Cohen, J. G., Christlieb, N., Qian, Y.-Z., et al. 2003, ApJ, 588, 1082
Cohen, J. G., McWilliam, A., Shectman, S., et al. 2006, AJ, 132, 137
Cowan, J. J, & Rose, W. K. 1977, ApJ, 212, 149
Cowperthwaite, P. S., Berger, E., Villar, V. A., et al. 2017, ApJ, 848, L17
De Smedt, K., Van Winckel, H., Kamath, D., & Wood, P. R. 2015, A&A, 583, A56
De Smedt, K., Van Winckel, H., Kamath, D., et al. 2016, A&A, 587, A6
Drout, M. R., Piro, A. L., Shappee, B. J., et al. 2017, Science, 358, 1570
Frebel, A., Christlieb, N., Norris, J. E., et al. 2007, ApJ, 660, L117
Gallino, R., Arlandini, C., Busso, M., et al. 1998, ApJ, 497, 388
Goswami, A., Aoki, W., Beers, T. C., et al. 2006, MNRAS, 372, 343
Hampel, M., Stancliffe, R. J., Lugaro, M., & Meyer, B. S. 2016, ApJ, 831, 171
Hayek, W., Wiesendahl, U., Christlieb, N., et al. 2009, A&A, 504, 511
Hill, V., Plez, B., Cayrel, R., et al. 2002, A&A, 387, 560
Ivans, I. I., Sneden, C., Gallino, R., Cowan, J. J., & Preston, G. W. 2005, ApJ, 627, L145
Ivans, I. I., Simmerer, J., Sneden, C., et al. 2006, ApJ, 645, 613
Ji, A. P., Frebel, A., Chiti, A., & Simon, J. D. 2016, Natur, 531, 610
Ji, A. P., &Frebel, A. 2018, ApJ, 856, 138
Johnson, J. A., & Bolte, M. 2004, ApJ, 605, 462
Jonsell, K., Barklem, P. S., Gustafsson, B., et al. 2006, A&A, 451, 651
Kamath, D., Wood, P. R., &Van Winckel, H. 2015, MNRAS, 454, 1468
Komiya, Y., & Shigeyama, T. 2016, ApJ, 830, 76
Lambert, D. L., Smith, V. V., Busso, M., Gallino, R., Straniero, O. 1995, ApJ 450, 302
Li, H.-J., Shen, X.-J.,Liang, Sh., Cui, W.-Y., Zhang, B. 2013a, PASP, 125, 143
Li, H.-J., Cui, W.-Y., Zhang, B. 2013b, ApJ, 775, 12
Masseron, T., Johnson, J. A., Plez, B., et al. 2010, A&A, 509, A93
Placco, V. M., Frebel, A., Beers, T. C., et al. 2013, ApJ, 770, 104
Placco, V. M., Holmbeck, E. M., Frebel, A., et al. 2017, ApJ, 844, 18
Preston, G. W., & Sneden, C. 2001, AJ, 122, 1545
Qian, Y.-Z., & Wasserburg, G. J. 2007, PhRe, 442, 237
Raiteri, C. M., Gallino, R., Busso, M., Neuberger, D., & Käppeler, F. 1993, ApJ, 419, 207
Reyniers, M., Van Winckel, H., Gallino, R., & Straniero, O. 2004, A&A, 417, 269
Roederer, I. U., Sakari, C. M., Placco, V. M., Beers, T. C., et al. 2018, ApJ, 865, 129
Smith, V. V., & Lambert, D. L. 1990, ApJS, 72, 387
Sneden, C., Cowan, J. J., Lawler, J. E., et al. 2003, ApJ, 591, 936
Tanvir, N. R., Levan, A. J., et al. 2017, ApJ, 848, L27
Timmes, F. X., Woosley, S. E., & Weaver, T. A. 1995, ApJS, 98, 617
Travaglio, C., Galli, D., Gallino, R., et al. 1999, ApJ, 521, 691
Travaglio, C., Gallino, R., Arnone, E., et al. 2004, ApJ, 601, 864
Tsujimoto, T., & Shigeyama, T. 2014, A&A, 565, L5
van Aarle, E., Van Winckel, H., De Smedt, K., Kamath, D., & Wood, P. R. 2013, A&A, 554, A106
Van der Swaelmen, M., Hill, V., Primas, F., Cole, A. A. 2013, A&A, 560, A44
Van Winckel, H., & Reyniers, M. 2000, A&A, 354, 135
Van Winckel, H. 2003, ARA&A, 41, 391
Yang, G.-C., Li, H.-J., Liu, N., Zhang, L., et al. 2017, PASP, 129, 064201